

# Elliptic flow of thermal dileptons as a probe of QCD matter

Payal Mohanty<sup>1</sup>, Victor Roy<sup>1</sup>, Sabyasachi Ghosh<sup>1</sup>, Santosh K Das<sup>1</sup>,

Bedangadas Mohanty<sup>2</sup>, Sourav Sarkar<sup>1</sup>, Jan-e Alam<sup>1</sup> and Asis K Chaudhuri<sup>1</sup>

<sup>1</sup> *Theoretical Physics Division, Variable Energy Cyclotron Centre, Kolkata 700064, India and*

<sup>2</sup> *Variable Energy Cyclotron Centre, Kolkata 700064, India*

(Dated: May 29, 2018)

We study the variation of elliptic flow of thermal dileptons with transverse momentum ( $p_T$ ) and invariant mass ( $M$ ) for Pb+Pb collisions at  $\sqrt{s_{NN}} = 2.76$  TeV for 30-40% centrality. The dilepton productions from quark gluon plasma (QGP) and hot hadrons have been considered including the spectral change of light vector mesons in the thermal bath. The space time evolution has been carried out within the framework of 2+1 dimensional ideal hydrodynamics with lattice+hadron resonance gas equation of state. We find that a judicious selection of  $M$  window can be used to extract the collective properties of quark matter, hadronic matter and also get a distinct signature of medium effects on vector mesons. Results within the ambit of the present work for nuclear collisions at Large Hadron Collider (LHC) indicate a reduction of elliptic flow ( $v_2$ ) for  $M$  beyond  $\phi$  mass, which if observed experimentally would imitate the small momentum anisotropy in the early stage of the collective motion of the partons. We also observe that the magnitude of the elliptic flow is significantly larger at LHC than at Relativistic Heavy Ion Collider (RHIC) collision conditions.

PACS numbers: 25.75.+r, 25.75.-q, 12.38.Mh

Collision between nuclei at relativistic energies provides an opportunity to study Quantum Chromodynamics (QCD) at non-zero temperatures and densities. Calculations based on lattice QCD (LQCD) predict that at high temperatures and/or densities hadronic matter melts down to a state of deconfined thermal quarks and gluons - a phase of matter called quark gluon plasma (QGP). The weakly interacting picture of the QGP stems from the perception of asymptotic freedom of QCD at high temperatures and densities. However, the LQCD calculations indicate that the deconfined system does not reach the Stefan-Boltzmann limit corresponding to the non-interacting massless gas of quarks, antiquarks and gluons even at a temperature as high as 1000 MeV [1]. The RHIC and LHC are the two experimental facilities where the QGP can be created by colliding nuclei at high energies. Several probes to study the properties of QGP have been proposed. Among those the azimuthal anisotropy or the elliptic flow ( $v_2$ ) of the produced particles have been shown to be sensitive to the initial condition and the equation of state (EoS) of the evolving matter formed in heavy ion collision (HIC)(see [2-4] for review).

Non-central heavy-ion collisions provide an anisotropic spatial configuration which together with the interactions among the constituents develop pressure gradients of different magnitude along different spatial directions. With the expansion the spatial anisotropy reduces and the momentum space anisotropy builds up rapidly. The  $v_2$  is a measure of this momentum space anisotropy which is defined as:  $v_2 = \langle \cos(2(\phi - \Psi)) \rangle = \langle p_x^2 - p_y^2 \rangle / \langle p_x^2 + p_y^2 \rangle$ , where  $p_x$  and  $p_y$  are the  $x$  and  $y$  component of the particle momenta,  $\phi$  is the azimuthal angle of the

produced particles and  $\Psi$  is the angle subtended by the plane containing the beam axis and impact parameter with  $x$ -direction. Comparison of measured  $v_2$  with those calculated using relativistic hydrodynamic and transport approaches have lead to several important results. The most important of these is the small shear viscosity to entropy ratio of the QGP compared to other known fluids [5]. The mass ordering of  $v_2$  of identified hadrons, clustering of  $v_2$  separately for baryons and mesons at intermediate  $p_T$  are considered as signatures of partonic coalescence as a mechanism of hadron production [6, 7]. In contrast to hadrons, which are predominantly emitted from the freeze-out surface of fireball, the electromagnetically interacting particles (real photons and lepton pairs) are considered as penetrating probes [8] (see Refs. [9-11] for review) which can carry information from the hot interior of the system. Therefore, the analysis of  $v_2$  of lepton pairs and photons can provide information of the pristine stage of the matter produced in HIC. The  $v_2$  of dileptons [12] and photons [13] have been evaluated for RHIC energies and shown that it can be used as effective probes to extract the properties of the partonic plasma. The sensitivity of  $v_2$  of lepton pairs on EoS has been elaborated in [14] for RHIC collision conditions. The lepton pairs are produced from each space time point of the system and hence the study of  $v_2$  of lepton pairs will shed light on the time evolution of collectivity in the system. Further, in addition to  $p_T$ , dileptons have an additional kinematic variable,  $M$  unlike photon. The evolution of radial flow can be estimated by studying the  $p_T$  spectra of lepton pairs for different  $M$  windows [15, 16]. The radial flow alters the shape of the  $p_T$  spectra of dileptons - it kicks

the low  $p_T$  pairs to the higher  $p_T$  domain, making the spectra flatter. Therefore, the presence of large radial flow may diminish the magnitude of  $v_2$  at low  $p_T$  [17] and this effect will be larger when the radial flow is large i.e. in the hadronic phase which corresponds to lepton pairs with  $M \sim m_\rho$ .

It has been argued that the anisotropic momentum distribution of the hadrons can bring the information on the interaction of the dense phase of the system [2] despite the fact that the hadrons are emitted from the freeze-out surfaces when the system is too dilute to support collectivity. Therefore, a suitable dynamical model is required to extrapolate the final hadronic spectra backward in time to get the information about the early dense phase. Such an extrapolation is not required for lepton pairs because they are emitted from the entire space-time volume of the system. Therefore, the  $v_2$  of lepton pairs provide information of the hot and dense phase directly. The  $v_2$  of dileptons can also be used to test the validity and efficiency of the extrapolation required for hadronic  $v_2$ . We will also see below that the  $p_T$  integrated  $M$  distribution of lepton pairs with  $M (> m_\phi)$  originate from the early time, providing information of the partonic phase and pairs with  $M \lesssim m_\rho$  are chiefly produced later from the hadronic phase. Therefore, the  $p_T$  integrated  $M$  distribution of lepton pairs may be used as a chronometer of the heavy ion collisions. On the other hand, the variation of  $v_2$  with  $p_T$  for different  $M$  windows may be used as a flow-meter.

In this work we study the  $M$  and  $p_T$  dependence of  $v_2$  for dileptons using relativistic ideal hydrodynamics [18] assuming boost invariance along the longitudinal direction [19] for LHC collision conditions. We argue that the  $v_2$  of lepton pairs from QGP and hadronic phases can be estimated with an appropriate choice of  $M$ . In addition to this we also show that the thermal effects on the  $\rho$  spectral function is visible through  $v_2$  in the low mass (below  $\rho$  peak) dileptons.

The elliptic flow of dilepton,  $v_2(p_T, M)$  can be defined as:

$$v_2 = \frac{\sum \int \cos(2\phi) \left( \frac{dN}{d^2 p_T dM^2 dy} \Big|_{y=0} \right) d\phi}{\sum \int \left( \frac{dN}{d^2 p_T dM^2 dy} \Big|_{y=0} \right) d\phi} \quad (1)$$

where the  $\sum$  stands for summation over Quark Matter(QM) and Hadronic Matter(HM) phases. The quantity  $dN/d^2 p_T dM^2 dy|_{y=0}$  appearing in Eq. 1 can be obtained from the dilepton production per unit four volume,  $dN/d^4 p d^4 x$  in a thermalized medium by integrating over the space-time evolution of the system. The quantity,  $dN/d^4 p d^4 x$  is given by [8]:

$$\frac{dN}{d^4 p d^4 x} = -\frac{\alpha^2}{6\pi^3} \frac{1}{M^2} L(M^2) \exp\left(-\frac{p_0}{T}\right) g^{\mu\nu} W_{\mu\nu}(p_0, \vec{p}) \quad (2)$$

where  $W_{\mu\nu}(p_0, \vec{p})$  is the electromagnetic (EM) current correlator,  $g^{\mu\nu}$  is the metric tensor,  $\alpha$  is the electromagnetic coupling,  $p = (p_0, \vec{p})$  is the four-momentum of the pair,  $T$  is the temperature of the thermal bath,  $L(M^2) = (1 + 2m_l^2/M^2) \sqrt{1 - 4m_l^2/M^2}$  arises from the Dirac spinors (lepton pair) in the final state,  $M$  is the invariant mass of the lepton pair and  $m_l$  is the lepton mass.

For QGP Eq. 2 leads to the standard rate of lepton pair production (in the leading order) from annihilation of  $q\bar{q}$  pairs [20]. For the dilepton production from hot hadrons we briefly outline the dilepton production processes here and refer to [21] for details. For the low mass dilepton production from HM the decays of thermal light vector mesons namely  $\rho$ ,  $\omega$  and  $\phi$  have been considered. The change of spectral function of  $\rho$  due to its interaction with  $\pi, \omega, a_1, h_1$  (see [21, 22] for details) and baryons [23] have been included in evaluating the production of lepton pairs from HM. For the  $\omega$  spectral function the width at non-zero temperature is taken from Ref [24] and medium effects on  $\phi$  is ignored here. The continuum part of the spectral function of  $\rho$  and  $\omega$  have also been included in dilepton production rate [10, 25]. In the present work dileptons from non-thermal sources *e.g.* from the Drell-Yan process and decays of heavy flavours [26] have been ignored in evaluating the elliptic flow of lepton pairs from QM and HM. If the charm and bottom quarks do not thermalize then they are not part of the flowing QGP and hence do not contribute to the elliptic flow. The model employed in the present work leads to a good agreement with NA60 dilepton data [27] for SPS collision conditions [28].

To evaluate  $v_2$  from Eq. 1 one needs to integrate the production rate given by Eq. 2 over the space time evolution of the system - from the initial QGP phase to the final hadronic freeze-out state through a phase transition in the intermediate stage. We assume that the matter is formed in QGP phase with negligible net baryon density. The initial condition required to solve the hydrodynamic equations for the description of the matter produced in Pb+Pb collision at  $\sqrt{s_{NN}} = 2.76$  TeV for 30-40% centrality are taken as follows:  $T_i = 456$  MeV is the value of the initial temperature corresponding to the maximum of the initial energy density profile at the thermalization time  $\tau_i = 0.6$  fm/c. The value of the transition temperature,  $T_c$  for quark hadron conversion is taken as 175 MeV. The EoS required to close the hydrodynamic equations is constructed by complementing Wuppertal-Budapest lattice simulation [1] with a hadron resonance gas comprising of all the hadronic resonances up to mass of 2.5 GeV [29, 30]. The energy of the lepton pair ( $p_0$ ) originating from a hydrodynamically expand-

ing system should be replaced by its value ( $p \cdot u$ ) in the co-moving frame which is given by:  $p \cdot u = \gamma_T(M_T \cosh(y - \eta) - v_x p_T \cos \phi - v_y p_T \sin \phi)$ , where  $u = (\gamma, \gamma \vec{v})$ , is the fluid four-velocity,  $y$  is the rapidity and  $\eta$  is the space-time rapidity,  $\gamma_T = (1 - v_T^2)^{-1/2}$ ,  $v_T^2 = v_x^2 + v_y^2$ ,  $v_x$  and  $v_y$  are the  $x$  and  $y$  component of the velocity. The system is assumed to get out of chemical equilibrium at  $T = T_{ch} = 170$  MeV [31]. The kinetic freeze-out temperature  $T_F = 130$  MeV is fixed from the  $p_T$  spectra of the produced hadrons at the same collision energy of Pb+Pb system. The EoS and the values of the parameters mentioned above are constrained by the  $p_T$  spectra (for 0 – 5% centrality) and elliptic flow (for 10 – 50% centrality) of charged hadrons [29] measured by ALICE collaboration [32].

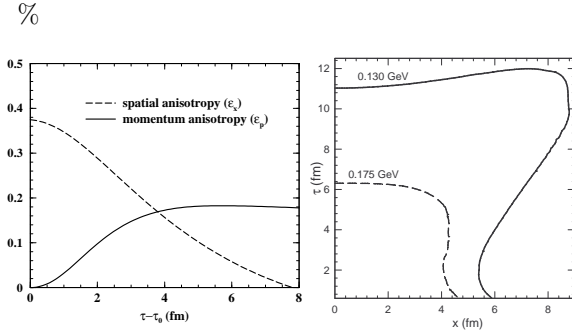


FIG. 1: Left panel: Variations of spatial and momentum space anisotropy with proper time. Right panel: Constant temperature contours denoting the space time boundaries of the QGP and hadronic phases.

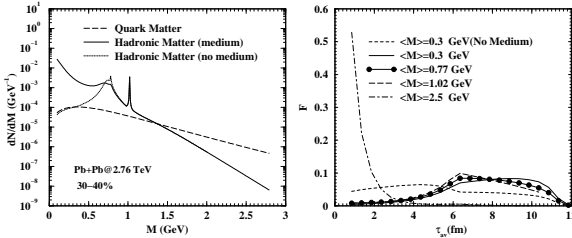


FIG. 2: Left panel: Invariant mass distribution of lepton pairs from quark matter and hadronic matter (with and without medium effects). Right panel: Fractional contribution of lepton pairs for various invariant mass windows as a function of average proper time (see text for details).

The spatial anisotropy of the matter produced in non-central HIC is defined as:  $\epsilon_x = \frac{\langle x^2 - y^2 \rangle}{\langle x^2 + y^2 \rangle}$ , where the average is taken over the energy distribution of the system formed in a collision of given impact parameter. The resulting momentum anisotropy of the interacting system produced in non-central HIC is

defined as:  $\epsilon_p = \frac{\int dx \int dy [T^{yy} - T^{xx}]}{\int dx \int dy [T^{yy} + T^{xx}]}$ , The variations of ( $\epsilon_x$ ) and ( $\epsilon_p$ ) with time have been displayed in the left panel of Fig. 1 for 30-40% centrality. We find that  $\epsilon_x$  ( $\epsilon_p$ ) reduces (increases) with time due to the prevailing pressure gradients which causes the matter to flow. Since  $v_2 \propto \epsilon_p$  therefore, the variations of  $v_2$  and  $\epsilon$  with  $\tau$  are expected to be similar. In Fig. 1 (right) we depict the constant temperature contours corresponding to  $T_c = 175$  MeV and  $T_f = 130$  MeV in the  $\tau - x$  plane (at zero abscissa) indicating the boundaries for the QM and HM phases respectively. The life time of the QM phase  $\sim 6$  fm/c and the duration of the HM is  $\sim 6 - 12$  fm/c. Throughout this work by early and late will approximately mean the duration of the QM and HM respectively.

With all the ingredients mentioned above we evaluate the  $p_T$  integrated  $M$  distribution of lepton pairs originating from QM and HM (with and without medium effects on the spectral functions of  $\rho$  and  $\omega$ ). The results are displayed in Fig. 2 (left) for the initial conditions and centrality mentioned above. We observe that for  $M > M_\phi$  the QM contributions dominate. For  $M_\rho \lesssim M \lesssim M_\phi$  the HM shines brighter than QM. For  $M < M_\rho$ , the HM (solid line) overshines the QM due to the enhanced contributions primarily from the medium induced broadening of  $\rho$  spectral function. However, the contributions from QM and HM become comparable in this region of  $M$  if the medium effects on  $\rho$  spectral function is ignored (dotted line). Therefore, the results depicted in Fig. 2 (left) indicate that a suitable choice of  $M$  window will enable us to unravel the contributions from a particular phase (QM or HM).

To further quantify these issues we evaluate the following quantity:

$$F = \frac{\int' \left( \frac{dN}{d^4x d^2p_T dM^2 dy} \right) dx dy d\eta \tau d\tau d^2p_T dM^2}{\int \left( \frac{dN}{d^4x d^2p_T dM^2 dy} \right) dx dy d\eta \tau d\tau d^2p_T dM^2} \quad (3)$$

where the  $M$  integration in both the numerator and denominator are performed for selective  $M$  windows from  $M_1$  to  $M_2$  with mean  $M$  defined as  $\langle M \rangle = (M_1 + M_2)/2$ . The prime in  $\int'$  in the numerator indicates that the  $\tau$  integration in the numerator is done from  $\tau_1 = \tau_i$  to  $\tau_2 = \tau_i + \Delta\tau$  with progressive increment of  $\Delta\tau$ , while in the denominator the integration is done over the entire lifetime of the system. In the right panel of Fig. 2,  $F$  is plotted against  $\tau_{av} = (\tau_1 + \tau_2)/2$ . The results substantiate the fact that pairs with high  $\langle M \rangle \sim 2.5$  GeV originate from QM ( $\tau_{av} \lesssim 6$  fm/c, QGP phase) and pairs with  $\langle M \rangle \sim 0.77$  GeV mostly emanate from the HM phase ( $\tau_{av} \geq 6$  fm/c). The change in the properties of  $\rho$  due to its interaction with thermal hadrons in the bath is also visible through  $F$  evaluated for  $\langle M \rangle \sim 0.3$  GeV with and without medium effects.

This clearly indicates that the  $\langle M \rangle$  distribution of lepton pairs can be exploited to extract collectivity of different phases of the evolving matter.

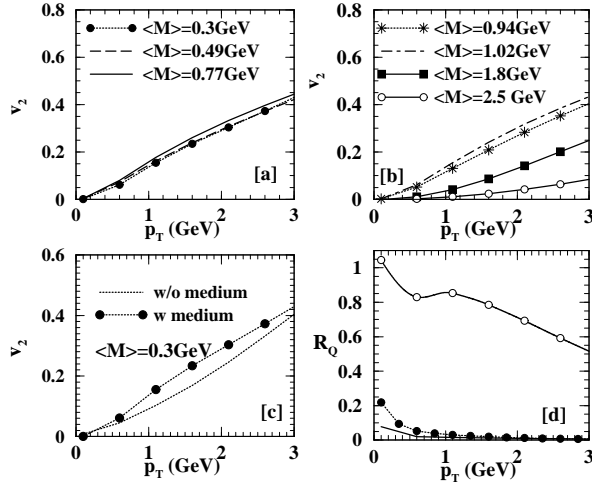


FIG. 3: [a] and [b] indicate elliptic flow of lepton pairs as a function of  $p_T$  for various  $M$  windows. [c] displays the effect of the broadening of  $\rho$  spectral function on the elliptic flow for  $\langle M \rangle = 300$  MeV. [d] shows the variation of  $R_Q$  (see text) with  $p_T$  for  $\langle M \rangle = 0.3$  GeV (solid circle),  $0.77$  GeV (line) and  $2.5$  GeV (open circle). All the results displayed here are for 30-40% centrality.

Fig. 3 ([a] and [b]) show the differential elliptic flow,  $v_2(p_T)$  of dileptons arising from various  $\langle M \rangle$  domains. We observe that for  $\langle M \rangle = 2.5$  GeV,  $v_2$  is small for the entire  $p_T$  range because these pairs arise dominantly from the QM epoch (see Fig. 2, right panel) when the flow is not developed fully. By the time (6-12 fm/c) when the pairs are emitted predominantly in the region  $\langle M \rangle = 0.77$  GeV, the flow is fully developed which gives rise to large  $v_2$ . It is also interesting to note that the medium induced enhancement of  $\rho$  spectral function provides a visible modification in  $v_2$  for dileptons below  $\rho$  peak (Fig. 3 [c]). The medium-induced effects lead to an enhancement of  $v_2$  of lepton pairs which is culminating from the ‘extra’ interaction (absent when a vacuum  $\rho$  is considered) of the  $\rho$  with other thermal hadrons in the bath. We note that the differential elliptic flow,  $v_2(p_T)$  obtained here at LHC is larger than the values obtained at RHIC [12, 14] for all the invariant mass windows. In Fig. 3 [d] we depict the variation of  $R_Q$  with  $p_T$  for  $\langle M \rangle = 0.3$  GeV (line with solid circle)  $0.77$  GeV (solid line) and  $2.5$  GeV (line with open circle). The quantity  $R_Q$  ( $R_H$ ) is defined as,  $R_Q = v_2^{QM} / (v_2^{QM} + v_2^{HM})$  [ $R_H = v_2^{HM} / (v_2^{QM} + v_2^{HM})$ ] where  $v_2^{QM}$  and  $v_2^{HM}$  are the elliptic flow of QM and HM respectively. The results clearly illustrate that  $v_2$  of lepton pairs in the large  $\langle M \rangle$  ( $= 2.5$  GeV) domain (open circle

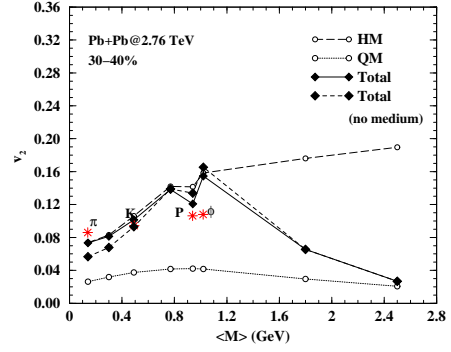


FIG. 4: (Color online) Variation of dilepton elliptic flow as function of  $\langle M \rangle$  for QM, HM (with and without medium effects) and for the entire evolution. The symbol \* indicates the value of  $v_2$  for hadrons *e.g.*  $\pi$ , kaon, proton and  $\phi$ .

in Fig. 3 [d]) originate from QM for the entire  $p_T$  range considered here. The value of  $R_Q$  is large in this domain because of the large (negligibly small) contributions from QM (HM) phase. It is also clear that the contribution from QM phase to the elliptic flow for  $\langle M \rangle (= 0.77$  GeV) is very small (solid line in Fig. 3 [d]). The value of  $R_H$  for  $\langle M \rangle = 0.77$  GeV is large (not shown in the figure).

The  $v_2$  at the HM phase (either at  $\rho$  or  $\phi$  peak) is larger than its value in the QGP phase (at  $\langle M \rangle = 2.5$  GeV, say) for the entire  $p_T$  range considered here. Therefore, the  $p_T$  integrated values of  $v_2$  should also retain this character at the corresponding values of  $\langle M \rangle$ , which is clearly observed in Fig. 4 which displays the variation of  $v_2(\langle M \rangle)$  with  $\langle M \rangle$ . The  $v_2$  ( $\propto \epsilon_p$ ) of QM is small because of the small pressure gradient in the QGP phase. The  $v_2$  resulting from hadronic phase has a peak around  $\rho$  pole indicating the full development of the flow in the HM phase. For  $\langle M \rangle > m_\phi$  the  $v_2$  obtained from the combined phases approach the value corresponding to the  $v_2$  for QGP. Therefore, measurement of  $v_2$  for large  $\langle M \rangle$  will bring information of the QGP phase at the earliest time of the evolution. It is important to note that the  $p_T$  integrated  $v_2(\langle M \rangle)$  of lepton pairs with  $\langle M \rangle \sim m_\pi, m_K$  is close to the hadronic  $v_2^\pi$  and  $v_2^K$  (symbol \* in Fig. 4) if the thermal effects on  $\rho$  properties are included. Exclusion of medium effects give lower  $v_2$  for lepton pairs compared to hadrons. The fact that the  $v_2$  of the (penetrating) lepton pairs are similar in magnitude to the  $v_2$  of hadrons for ( $\langle M \rangle \sim m_\pi, m_K, m_{proton}$  etc), it ascertains that the anisotropic momentum distribution of hadrons carry the information of the HM phase with duration  $\sim 6-12$  fm/c (left panel of Fig. 1). We also observe that the variation of  $v_2(\langle M \rangle)$  with  $\langle M \rangle$  has a structure similar to  $dN/dM$  vs  $M$ . As indicated

by Eq. 1 we can write  $v_2(\langle M \rangle) \sim \sum_{i=QM, HM} v_2^i \times f_i$ , where  $f_i$  is the fraction of QM or HM from various space-time regions. The structure of  $dN/dM$  is reflected in  $v_2(\langle M \rangle)$  through  $f_i$ . We find that the magnitude of  $v_2(\langle M \rangle)$  at LHC is larger than its value at RHIC.

In conclusion, we have evaluated the  $v_2$  of dileptons originating from the Pb+Pb collisions at  $\sqrt{s_{NN}} = 2.76$  TeV for 30–40% centrality. Our study shows that  $v_2(M)$  provides useful information on the collective motion of the evolving QCD matter formed in high energy heavy-ion collisions. If the heavy quarks (charm and bottom) produced in HIC do not thermalize and hence not become part of the flowing QGP then the lepton pairs which originate from the decays of heavy flavours will not contribute to the  $v_2$  of lepton pairs. In such a scenario an experimental observation of the reduction of  $v_2(M)$  with increasing  $M$  beyond  $\phi$  mass would reflect the presence of

small momentum space anisotropy through modest collective motion in the QM phase. We observe that  $v_2(\langle M \rangle)$  of the penetrating probe (lepton pairs) for  $\langle M \rangle = m_\pi$  and  $m_K$  is similar to the hadronic  $v_2^\pi$  and  $v_2^K$  when the medium induced change in the  $\rho$  spectral function is included in evaluating the dilepton spectra. The medium effects are large during the dense phase of the hadronic system, therefore, this validates the findings that the hadronic  $v_2$  carry the information of the dense part of the hadronic phase. Our study also establishes the fact that the invariant mass dependence of dilepton  $v_2$  can in principle act as a clock for the space time evolution of the system formed in HIC.

**Acknowledgment:** PM, SKD and JA are partially supported by DAE-BRNS project Sanction No. 2005/21/5-BRNS/2455. BM is partially supported by DAE-BRNS project Sanction No. 2010/21/15-BRNS/2026.

- 
- [1] S. Borsanyi *et al.* JHEP **1011**, 077 (2010).  
 [2] P. Huovinen and P. V. Ruuskanen, Ann. Rev. Nucl. Part. Sci. **56**, 163 (2006).  
 [3] D. A. Teaney, arXiv:0905.2433 [nucl-th].  
 [4] T. Hirano, N. van der Kolk and A. Bilandzic, The Physics of the Quark-Gluon Plasma, Eds. S. Sarkar, H. Satz, B. Sinha, Springer, Heidelberg, 2009.  
 [5] R. Averbeck (for the PHENIX Collaboration), J. Phys. G **35**, 104115 (2008).  
 [6] STAR Collaboration, B. I. Abelev *et al.*, Phys. Rev. C **77**, 054901 (2007).  
 [7] PHENIX Collaboration, A. Adare *et al.*, Phys. Rev. Lett. **98**, 162301 (2007).  
 [8] L. D. McLerran and T. Toimela, Phys. Rev. D **31**, 545 (1985).  
 [9] J. Alam, S. Raha and B. Sinha, Phys. Rep. **273**, 243 (1996).  
 [10] J. Alam, S. Sarkar, P. Roy, T. Hatsuda and B. Sinha, Ann. Phys. **286**, 159 (2001).  
 [11] R. Rapp and J. Wambach, Adv. Nucl. Phys. **25**, 1 (2000).  
 [12] R. Chatterjee, D. K. Srivastava, U. W. Heinz and C. Gale, Phys. Rev. C **75**, 054909 (2007).  
 [13] R. Chatterjee, E. S. Frodermann, U. W. Heinz and D. K. Srivastava, Phys. Rev. Lett. **96**, 202302 (2006).  
 [14] J. Deng, Q. Wang, N. Xu and P. Zhuang, Phys. Lett. B **701**, 581 (2011).  
 [15] T. Renk and J. Ruppert, Phys. Rev. C **77**, 024907 (2008).  
 [16] J. K. Nayak and J. Alam, Phys. Rev. C **80**, 064906 (2009); P. Mohanty, J. K. Nayak, J. Alam and S. K. Das, Phys. Rev. C **82**, 034901 (2010); P. Mohanty, J. Alam and B. Mohanty, Phys. Rev. C **84**, 024903 (2011).  
 [17] P. Huovinen, P. F. Kolb, U. Heinz, P. V. Ruuskanen and S. A. Voloshin, Phys. Lett. B **503**, 58 (2001).  
 [18] P. F. Kolb, J. Sollfrank and U. Heinz, Phys. Rev. C **62**, 05 4909 (2000); P. F. Kolb and R. Rapp, Phys. Rev. C **67**, 044903 (2003); P. F. Kolb and U. Heinz, nucl-th/0305084, J. Sollfrank, P. Koch and U. Heinz, Phys. Lett. B **252**, 256 (1990) J. Sollfrank, P. Koch and U. Heinz, Z. Phys. C **52**, 593 (1991).  
 [19] J. D. Bjorken, Phys. Rev. D **27**, 140 (1983).  
 [20] J. Cleymans, J. Fingberg and K. Redlich, Phys. Rev. D **35**, 2153 (1987).  
 [21] S. Ghosh, S. Sarkar and J. Alam, Eur. Phys. J. C **71**, 176 (2011).  
 [22] S. Ghosh, S. Mallik and S. Sarkar, Eur. Phys. J. C **70**, 251 (2010).  
 [23] V. L. Eletsky, M. Belkacem, P. J. Ellis and J. I. Kapusta, Phys. Rev. C **64**, 035202 (2001).  
 [24] R. A. Schneider and W. Weise, Phys. Lett. B **515**, 89 (2001).  
 [25] E. V. Shuryak, Rev. Mod. Phys. **65**, 1 (1993).  
 [26] H. van Hess and R. Rapp, J. Phys. G **35**, 054001 (2008).  
 [27] R. Arnaldi *et al.* for NA60 Collaboration, Phys. Rev. Lett. **96**, 162302 (2006); Phys. Rev. Lett. **100**, 022302 (2008).  
 [28] J. K. Nayak, J. Alam, T. Hirano, S. Sarkar and B. Sinha, arXiv:0902.0446 [nucl-th]  
 [29] V. Roy, A. K. Choudhuri, Phys. Lett. B, **703**, 313 (2011).  
 [30] B. Mohanty and J. Alam, Phys. Rev. C **68**, 064903 (2003).  
 [31] T. Hirano and K. Tsuda, Phys. Rev. C **66**, 054905 (2002).  
 [32] K. Aamodt *et al.* [ALICE Collaboration], Phys. Rev. Lett. **106**, 032301 (2011); Phys. Lett. B **696**, 30 (2011).